PHYSICAL REVIEW B VOLUME 50, NUMBER 6 1 AUGUST 1994-II

^{93}Nb NMR in the incommensurate and quasicommensurate phases of barium sodium niobate

James A. Norcross and David C. Ailion
Department of Physics, University of Utah, Salt Lake City, Utah 84112

R. Blinc, J. Dolinsek, T. Apih, and J. Slak
Jozef Stefan Institute, University of Ljubljana, Ljubljana, Slovenia
(Received 4 April 1994)

NMR spectra have been measured for the quadrupole perturbed $\frac{1}{2}\rightarrow -\frac{1}{2}$ transition of ^{93}Nb in barium sodium niobate (BSN) between 300 and 650 K. The spectra are inhomogeneously broadened in the incommensurate (I) phase between $T_I=580$ K and $T_c=540$ K as well as in the quasicommensurate (QC) phase below T_c. However, the observed line shapes do not exhibit the characteristics of the lines for other $1q$ and $2q$ modulated incommensurate materials. The temperature dependence of the observed line shape can be explained using a model in which phase fluctuations induced by random, weak pinning of the modulation wave by defects produce Gaussian line broadening. Random pinning of the modulation wave also creates a large phason gap which makes spin-lattice relaxation via phasons inefficient. These results suggest that the presence of defects due to nonstoichiometry causes the I and QC phases of BSN to be "chaotic."

I. INTRODUCTION

Among incommensurate insulating materials, barium sodium niobate [$Ba_2NaNb_5O_{15}$ (BSN)] occupies an exceptional place. The order parameter for the transition from the tetragonal ferroelectric normal (N) phase to the incommensurate (I) phase at $T_I=580$ K has four components[1]

$$\eta_{\pm}=\rho_1 e^{\pm i\varphi_1} \tag{1a}$$

and

$$\xi_{\pm}=\rho_2 e^{\pm i\varphi_2}, \tag{1b}$$

and not just two as do most other I systems.[1] In the high-temperature I phase between $T_I=580$ K and $T_c=540$ K as well as in the orthorhombic phase below T_c, only one pair of order parameter components freezes out (either $\rho_1\neq 0$, $\rho_2=0$, or $\rho_2\neq 0$, $\rho_1=0$), resulting in the formation of orthorhombic domains with mutually perpendicular $1-q$ modulation directions, corresponding to the so-called "stripe" phase. The excitation spectrum should exhibit four modes: an amplitudon and a phason mode associated with the frozen-out one-dimensional modulation wave and a doubly degenerate soft mode connected with the pair of order parameter components which are not frozen out. The existence of the stripe phase produces a point symmetry change at the normal-to-incommensurate (N-I) transition which does not occur in most other N-I transitions. Another way in which BSN differs from most other incommensurate systems is that the phase below T_c is not perfectly commensurate and residual incommensurability exists down to 15 K.[2] Therefore the phase below T_c is usually designated as "quasicommensurate" (QC).

The width of the incommensurate and quasicommensurate satellites[3] and the birefringence[4] in BSN exhibit striking thermal hysteresis and relaxation effects. In contrast to Rb_2ZnCl_4, where broadening of the incommensurate satellites has been observed by Mashiyama, Tanisaki, and Hamano[3] in the multisoliton lattice regime near the "lock-in" transition at T_c, in BSN the broadening persists throughout the incommensurate and quasicommensurate phases. It is believed[5] that these memory and hysteresis effects are connected with the interaction between mobile point defects and the incommensurate modulation wave. One possibility is that the defects diffuse toward structural sites where the modulation wave has a particular phase, resulting in a pinning of the phase of the modulation wave. An alternative explanation is that a nonuniform distribution of these defects affects the periodicity of the modulation wave. At sufficiently high temperatures in the N phase, a uniform pattern of defect positions is restored after some time via thermally activated diffusion.

BSN has the tungsten-bronze structure consisting of a lattice of corner-sharing oxygen tetrahedra forming two types of tunnels in which the barium and sodium ions are located. There are five nonequivalent Nb sites.[6] The composition of BSN is generally nonstoichiometric,[7] and the main structural defect introduced by the nonstoichiometry is the occurrence of vacancies at the sodium sites. The nonstoichiometry of BSN also causes the transition temperatures T_I and T_c to vary from sample to sample. The incommensurate modulation consists primarily of a collective shearing of the oxygen octahedra. This modulation should strongly influence the electric field gradient (EFG) tensor at the sites of the covalently bonded Nb; therefore ^{93}Nb ($I=\frac{9}{2}$) NMR should be useful in revealing the local properties of the quasicommensurate and incommensurate phases of BSN.

0163-1829/94/50(6)/3625(6)/$06.00

II. THEORY

A. Effect of thermal fluctuations on the NMR line shape

Since the incommensurate and quasicommensurate phases of BSN occur at rather high temperatures, the effects of thermal fluctuations of the modulation wave phase on the NMR spectra have to be considered. We assume that the ^{93}Nb quadrupole-perturbed NMR frequency of a nucleus at a site (x,y,z) is a linear function of the nuclear displacements connected with the incommensurate modulation:

$$\omega(x,y,t)=\omega_0+a\eta(x,t)+b\xi(y,t)$$
$$=\omega_0+a[\eta_1(x,t)\cos(k_1x)+\eta_2(x,t)\sin(k_1x)]$$
$$+b\xi_\pm(y,t)[\cos(k_2y)+\sin(k_2y)] , \quad (2)$$

where

$$\eta_1(x,t)=\eta_{1E}+\eta_1'(x,t) , \quad (3a)$$

$$\eta_2(x,t)=\eta_2'(x,t) , \quad \eta_{2E}=0 , \quad (3b)$$

$$\xi_\pm(y,t)=\xi_\pm'(y,t) , \quad \xi_{1E}=\xi_{2E}=0 . \quad (3c)$$

Here η_{1E} represents the amplitude of the frozen-out one-dimensional modulation wave and $\eta_1'(x,t)$, $\eta_2'(x,t)$ represent the amplitude and phase fluctuations of this wave. $\xi_\pm(y,t)$ describes the doubly degenerate soft-mode fluctuations of the order parameter components which are not frozen.

The adiabatic NMR line shape $I(\omega)$ is

$$I(\omega)=\int_0^\infty G(t)e^{i\omega t}dt , \quad (4)$$

where

$$G(t)=e^{-i\omega_0 t}\left\langle\!\left\langle \exp\left[i\int_0^t[\omega(x,y,t')-\omega_0]dt'\right]\right\rangle\!\right\rangle . \quad (5)$$

The inner brackets represent a thermodynamic ensemble average, and the outer brackets represent a spatial average over the static inhomogeneous distribution of resonance frequencies.

It has been shown[8] that $G(t)$ can be expressed as

$$G(t)=e^{-i\omega_0 t}\langle\langle G_1(t)G_2(t)\rangle\rangle , \quad (6)$$

where

$$G_1(t)=e^{-i\omega_1\cos(k_1x)t} , \quad \omega_1=a\eta_{1E} , \quad (7)$$

represents the effects of the frozen-out static modulation wave and

$$G_2(t)=\exp\left[-ia\int_0^t[\eta_1'(x,t)\cos(k_1x)+\eta_2'(x,t)\sin(k_1x)]dt'\right]\exp\left[-ib\int_0^t\xi_\pm(y,t)[\cos(k_2y)+\sin(k_2y)]dt'\right] \quad (8)$$

describes the effects of thermal fluctuations. If one assumes that the effect of thermal fluctuations is negligible so that $G_2(t)\approx 1$, one gets from (4) and (7) the static incommensurate line shape

$$I(\omega)=\frac{1}{\sqrt{1-[(\omega-\omega_0)/\omega_1]^2}} , \quad (9)$$

showing the characteristic edge singularities at $\omega-\omega_0=\pm\omega_1$ [Fig. 1(a)]. The effect of thermal fluctuations can be described by convoluting $I(\omega)$ with the homogeneous quasi-Lorentzian line shape, which is the Fourier transform of $G_2(t)$, resulting in a line shape $F(\omega)$ given by

$$F(\omega)=\int I(\omega')L(\omega-\omega')d\omega' . \quad (10)$$

For large enough thermal fluctuations, the incommensurate splitting will be averaged out. The treatment is similar if the relation between the nuclear frequency and the displacement is quadratic. In this case one finds the static incommensurate lineshape to be

$$I(\omega)=\frac{\text{const}}{\sqrt{(\omega_0+\omega_2-\omega)(\omega-\omega_0)}} , \quad \omega_2=a\eta_{1E}^2 , \quad (11)$$

with singularities at $\omega-\omega_0=0$ and $\omega-\omega_0=\omega_2$ [Fig. 1(b)]. Here too, large thermal fluctuations will result in an averaging out of the characteristic incommensurate line shape.

In the special case that all four order parameter components freeze out, the result is a $2-q$ modulated "quilt" phase with a line shape given by a convolution of two $1-q$ frequency distributions:[9]

$$I(\omega)=\int_{-\infty}^{\infty}I_1(\omega')I_2(\omega-\omega')d\omega' , \quad (12)$$

where $I_1(\omega')$ and $I_2(\omega-\omega')$ are given by (9) for the linear case. If the amplitudes of the two modulation waves are equal so that ω_1 is the same for I_1 and I_2, the resulting line shape[9] has a logarithmic singularity at $\omega-\omega_0=0$ and two-step discontinuities at $\omega-\omega_0=\pm\omega_1$ [Fig. 1(c)].

B. Impurity effects

The previous treatment is appropriate for a perfect crystal without defects. Since the nonstoichiometry in BSN introduces mobile defects which pin the modulation wave, the ^{93}Nb NMR spectrum in BSN is expected to be quite different from that predicted by Eqs. (9)–(11).

The presence of defects will induce both strains and random fluctuations of the phase of the modulation wave around the plane wave value. As a result, there will be an additional Gaussian contribution to the width of individual lines:

$$\tilde{L}(\omega-\omega')=Ce^{-[(\omega-\omega')^2/2\sigma^2]} , \quad (13)$$

where

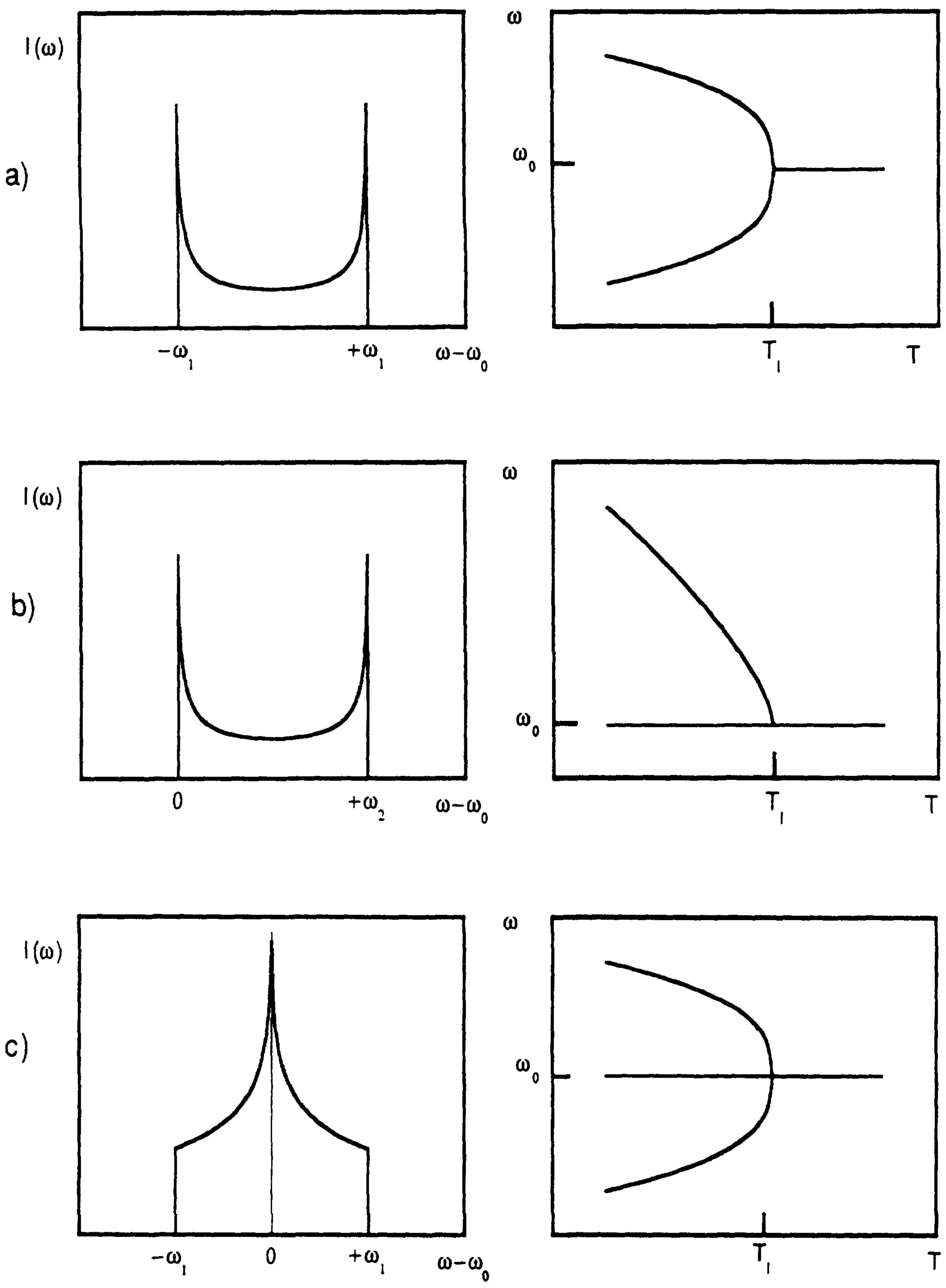

FIG. 1. Incommensurate line shapes $I(\omega)$ and the temperature dependence of discontinuities in $I(\omega)$ for (a) linear stripe, (b) quadratic stripe, and (c) linear quilt type modulations.

$$\sigma^2=\sigma_0^2+\sigma_{\rm ph}^2 \ . \tag{14}$$

Here σ_0^2 describes the weakly temperature-dependent random strain contribution to the line broadening, while $\sigma_{\rm ph}^2$ describes the phase fluctuation contribution. For the case when the relationship between the NMR [or nuclear quadrupole resonance (NQR)] frequency and the displacement is linear, one finds[10]

$$\sigma_{\rm ph}^2=\tfrac{1}{2}\omega_1^2\overline{\delta\varphi^2} \ . \tag{15}$$

Using the results obtained for $(Rb_{1-x}K_x)_2ZnCl_4$ crystals,[10] we obtain

$$\overline{\delta\varphi^2}=Kn_i\overline{\varphi_0^2} \ , \tag{16}$$

where K is a numerical factor of the order of 1, n_i is the concentration of defects, and $\overline{\varphi_0^2}$ is the mean-square phase deviation from the plane-wave value induced by a given defect. In Ref. 10, $\sigma_{\rm ph}^2$ is shown to have a temperature dependence given by

$$\sigma_{\rm ph}^2 \propto (T_I-T)^{(2n-2)\beta} \ . \tag{17}$$

For BSN, the commensurability index is $n=4$ and $\beta\approx 0.33$ is the critical exponent for the amplitude of the

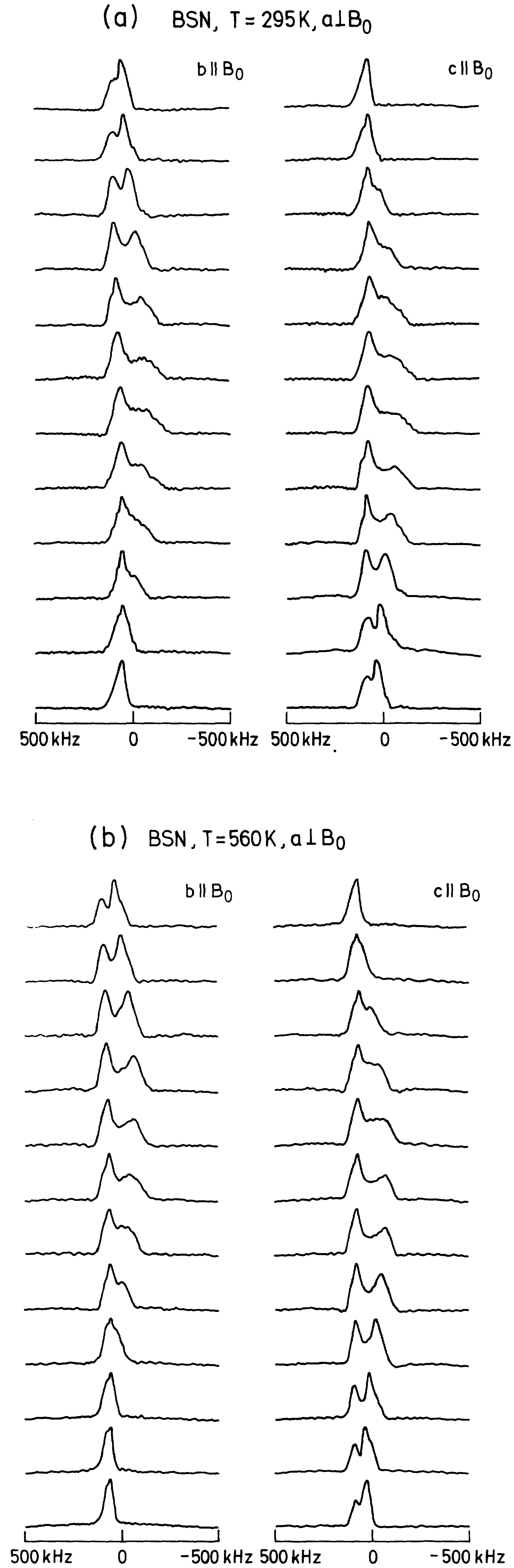

FIG. 2. Angular dependence of the ^{93}Nb central transition for rotations about the a axis in 7.5° increments. Results are for temperatures of (a) 295 K and (b) 560 K.

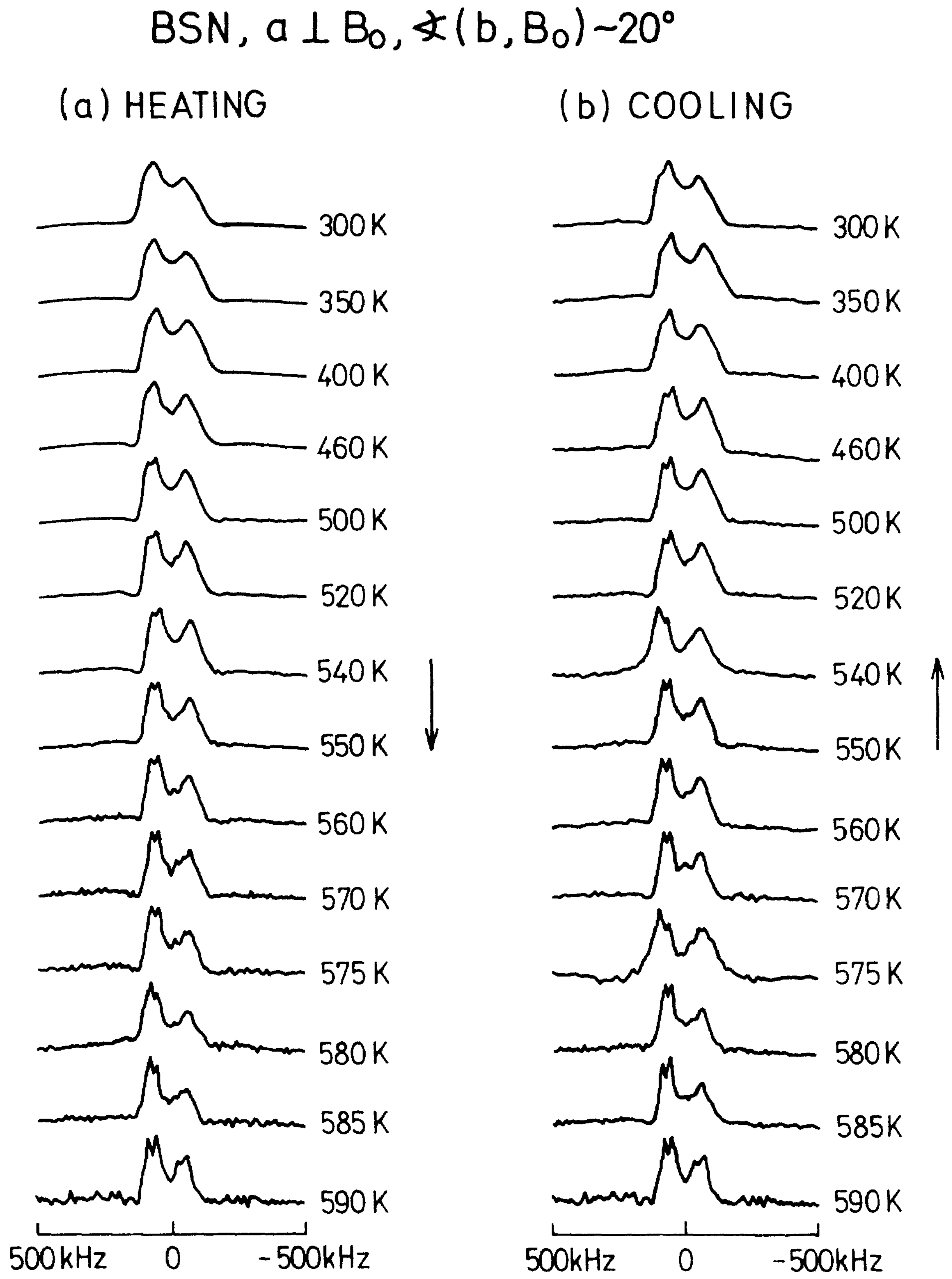

FIG. 3. Temperature dependence of the ^{93}Nb central transition for both (a) heating and (b) cooling cycles for $a \perp \mathbf{H}_0$, $<\mathbf{b}$, $\mathbf{H}_0 = 20°$.

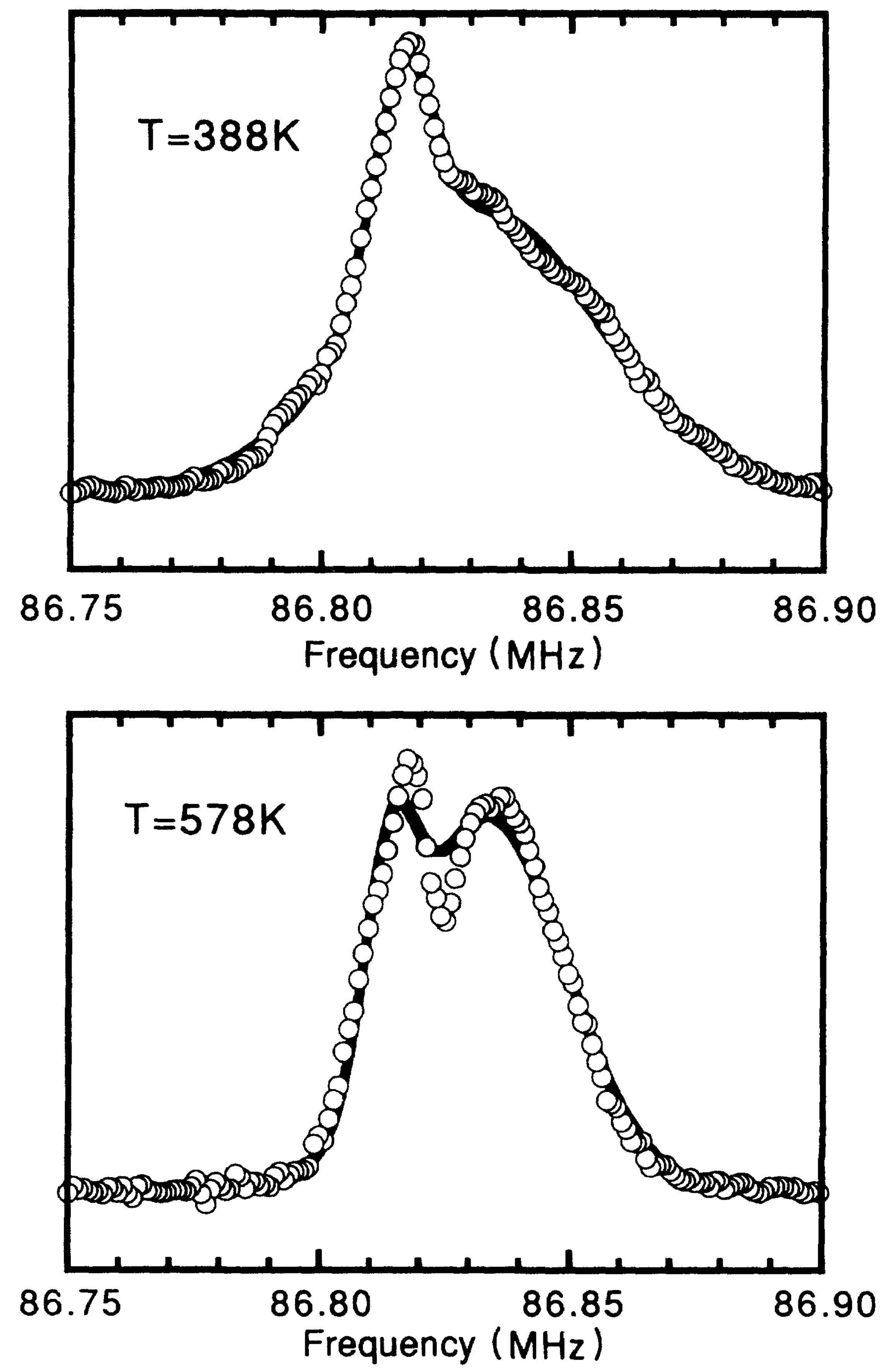

FIG. 5. Two-Gaussian fit of the ^{93}Nb line shape at 8.5 T for $\mathbf{H}_0 \| c$. The open circles are the experimental data, and the solid line is the theoretical fit.

frozen-out modulation wave. Thus σ_{ph} is expected to increase linearly with decreasing temperature [i.e., $\sigma_{ph} \propto (T_I - T)$].

The complete ^{93}Nb NMR spectrum will be

$$f(\omega) = \int F(w'')\tilde{L}(\omega - \omega'')d\omega'' , \tag{18}$$

a convolution of the static incommensurate line shape with both a Lorentzian line shape that describes thermal fluctuations and a Gaussian that describes random strain effects as well as effects due to the random pinning of the modulation wave by defects.

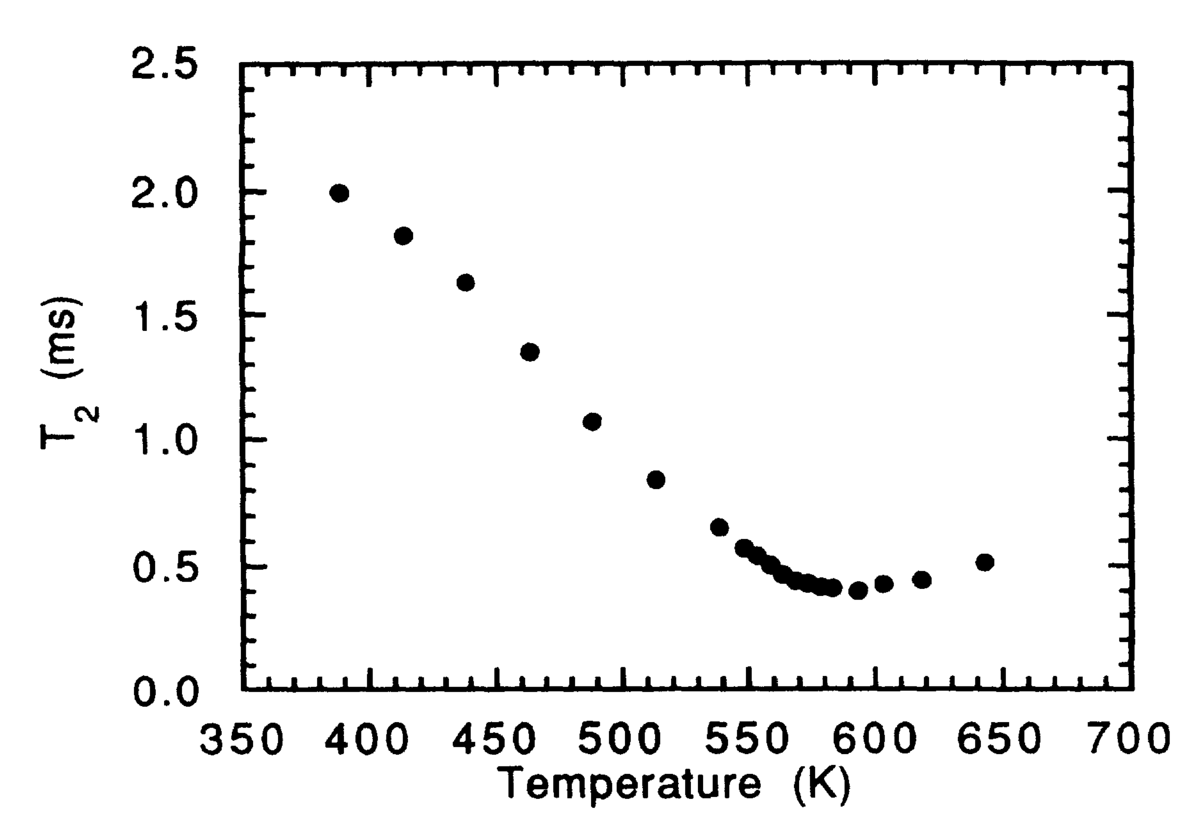

FIG. 4. Temperature dependence of the ^{93}Nb T_2 at 8.5 T for $\mathbf{H}_0 \| c$.

III. EXPERIMENTAL RESULTS AND DISCUSSION

Quadrupole-perturbed NMR line shapes are shown in Figs. 2 and 3 for the central transition of ^{93}Nb in a BSN single crystal. Figure 2 shows the angular dependence of

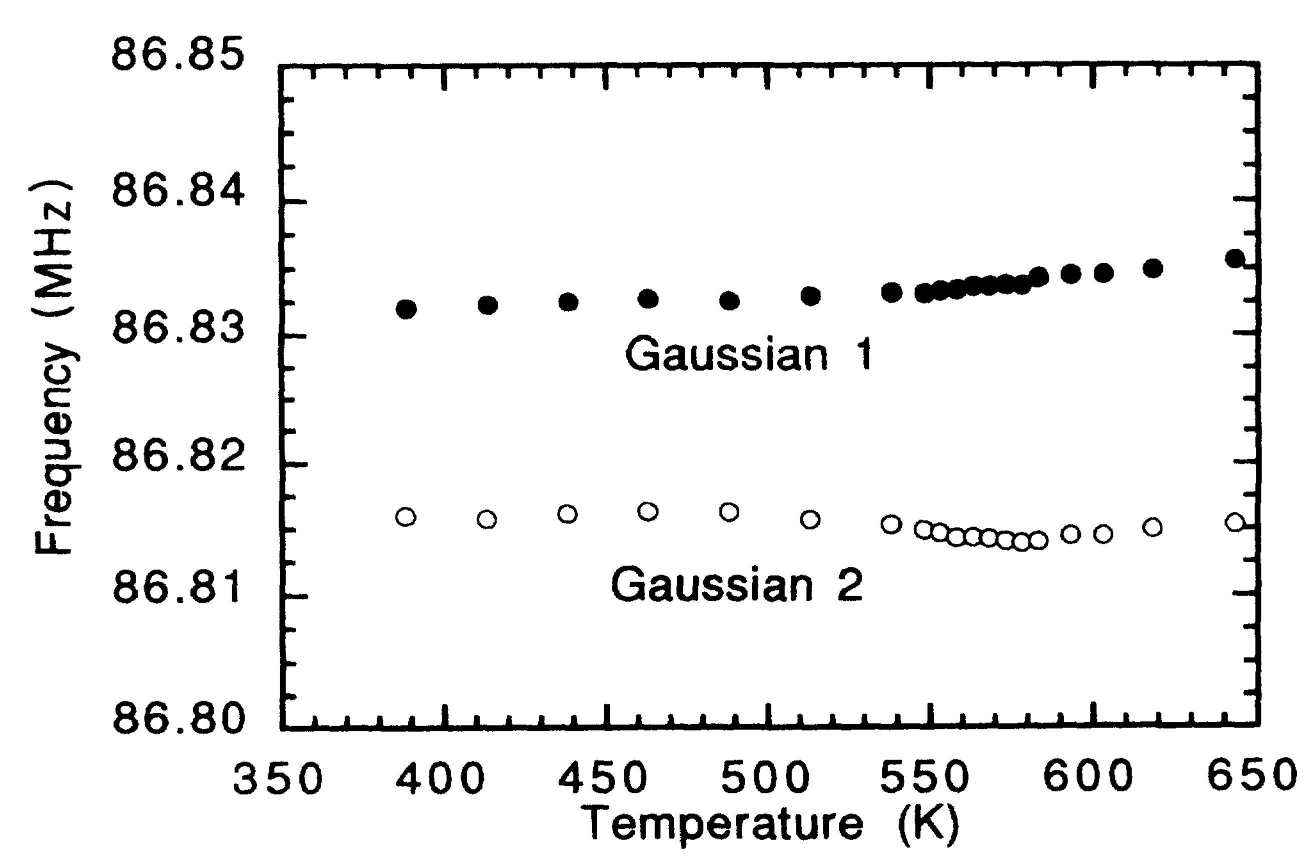

FIG. 6. Temperature dependence of the centers of two Gaussians obtained in a fit of the ^{93}Nb line shape at 8.5 T for $\mathbf{H}_0 \| c$.

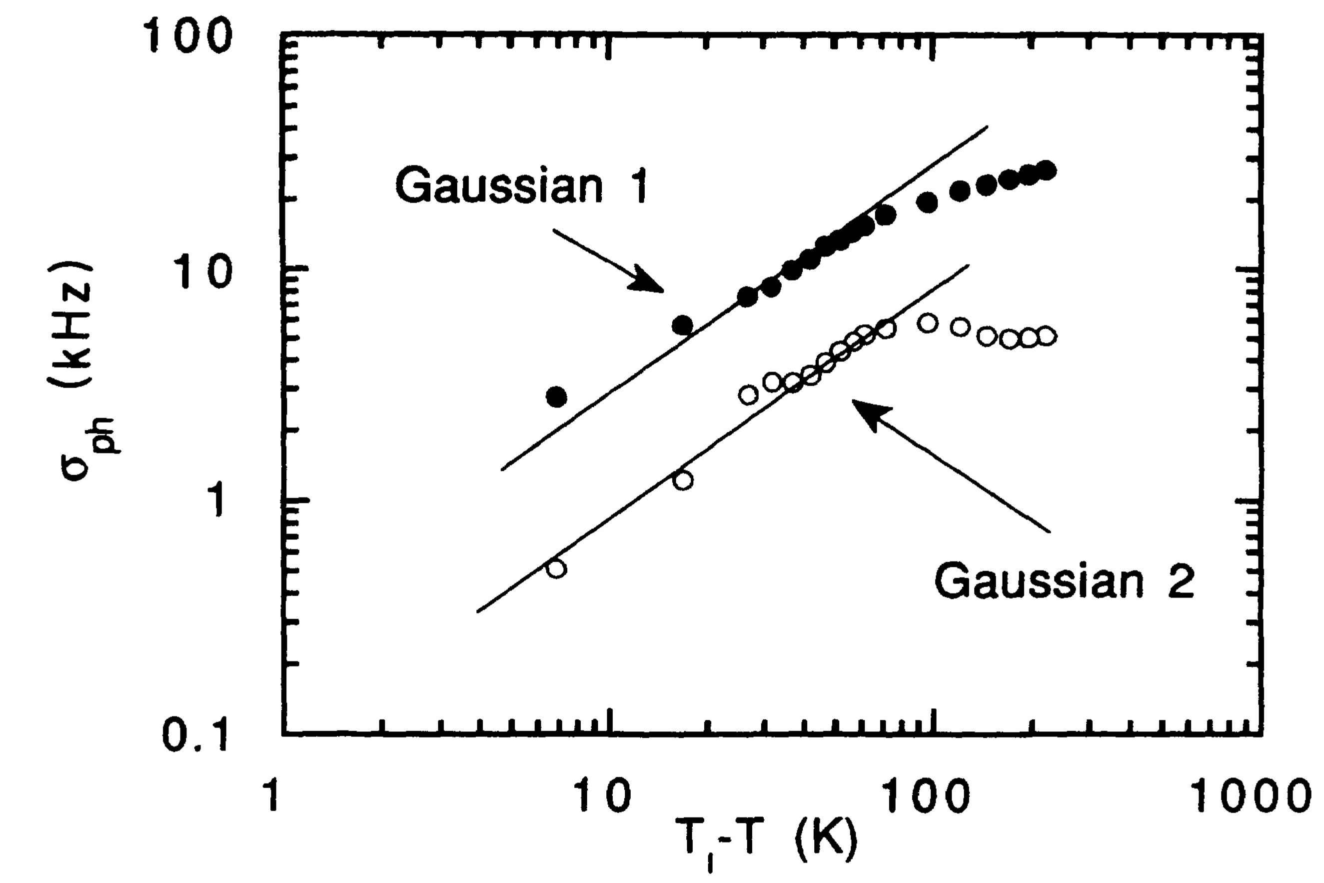

FIG. 7. Temperature dependence of σ_{ph}. The solid lines have slope one on the log-log scale.

the central transition for rotations about the a axis at temperatures of 295 and 560 K. Two broad overlapping lines are evident at 295 K, and additional structure appears at higher temperatures for certain orientations. Figure 3 shows the temperature dependence of the spectra for both heating and cooling cycles. The fine structure evident in the high-temperature ferroelectric phase above 573 K slowly disappears on cooling into the incommensurate and lower-temperature quasicommensurate phases. No significant difference in the spectra was observed for heating and cooling cycles.

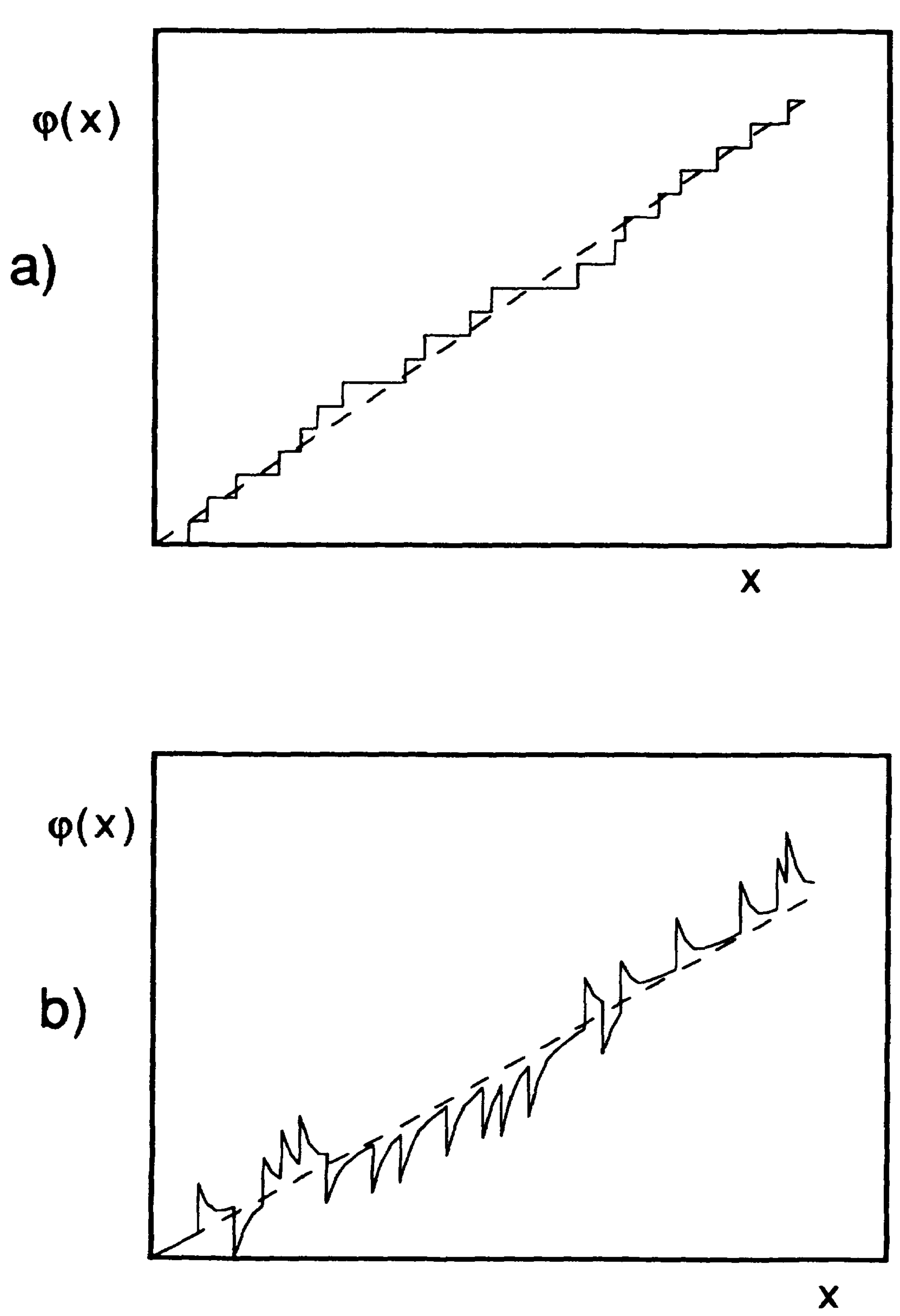

FIG. 8. Phase fluctuations in the chaotic state of (a) a pure incommensurate system and (b) an incommensurate system with impurities.

At no orientation does the observed line shape correspond to the stripelike [Figs. 1(a) and 1(b)] or quiltlike [Fig. 1(c)] modulated line shapes expected for the incommensurate phase. Measurements of the Hahn T_2 indicate that the lines are inhomogeneously broadened (Fig. 4). This result shows that the absence of the expected $1q$ or $2q$ fine structure (Fig. 1) is not due to motional averaging of the incommensurability by thermal fluctuations.

The observed temperature dependence of the spectra can, however, be explained by random pinning of the modulation wave by defects, with the resulting Gaussian broadening of the lines due to defect-induced phase fluctuations. The observed ^{93}Nb line shapes for $\mathbf{H}_0$ parallel to c (Fig. 5) can indeed be described by a superposition of two Guassians. Even though the centers of the Gaussians vary little with temperature (Fig. 6), the widths increase dramatically on going from the high-temperature ferroelectric phase to the incommensurate and quasicommensurate phases. The phase fluctuation contribution σ_{ph}^2 is obtained from Eq. (14) by taking σ_0 to be the high-temperature linewidth. According to the discussion following Eq. (17), σ_{ph} should be proportional to $T_I - T$. A plot of $\log\sigma_{ph}$ vs $\log(T_I - T)$ yields a straight line of unity slope over the incommensurate region (Fig. 7) as predicted, provided that T_I is taken to be 610 K. The observed increase in σ_{ph} in the incommensurate phase reflects the increase in the amplitude of the modulation wave, since

$$\sigma_{ph}^2 \propto A^{2n-2} . \qquad (19)$$

The fact that σ_{ph} is large and relatively temperature independent in the quasicommensurate phase agrees with previous observations[11] that randomly pinned solitons remain frozen in this phase.

Our data suggest that the entire incommensurate and quasicommensurate phases are "chaotic" due to point defects induced by the nonstoichiometry of the sample. It is well known that a chaotic phase[12,13] appears in pure systems just above T_c, where the intersoliton interaction becomes weak compared to the soliton-lattice coupling,

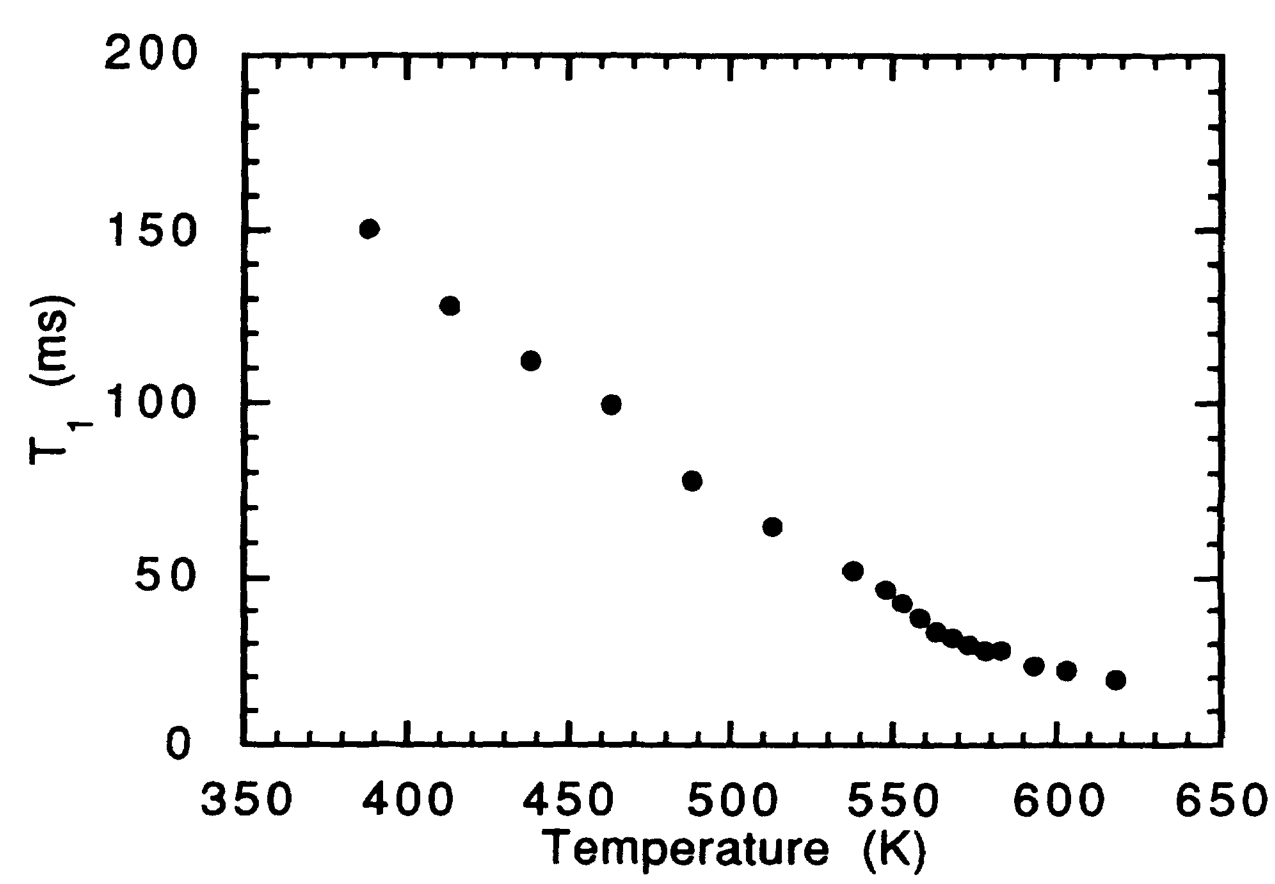

FIG. 9. Temperature dependence of T_1 of ^{93}Nb at 8.5 T for $\mathbf{H}_0 \| c$.

leading to a breakup of the multisoliton lattice and random pinning of solitons [Fig. 8(a)]. Such a phase has been observed previously in Rb_2ZnCl_4 close to the lock-in transition[13] as well as in substitutionally disordered $(Rb_{1-x}K_x)_2ZnCl_4$.[14] In BSN, the defect-induced chaotic phase occurs in the plane-wave regime. Also, defects should induce phase fluctuations which decay with distance from the defect,[10] as illustrated in Fig. 8(b). Thus the chaotic phase in BSN is quite different from that in pure systems.

The chaotic nature of the incommensurate and quasicommensurate phases is also responsible for the absence of another characteristic property of the classical incommensurate phase—a short, temperature-independent phason-induced spin-lattice relaxation time in the incommensurate phase. Figure 9 shows that the ^{93}Nb T_1 increases monotonically with decreasing temperature. The absence of the temperature-independent phason contribution to the spin-lattice relaxation is due to the fact that random pinning of the modulation wave induces a large phason gap Δ_φ which makes inefficient the spin-lattice relaxation via phasons,

$$\frac{1}{T_1}=\frac{K}{\Delta_\varphi}\,, \tag{20}$$

so that other mechanisms determine T_1.

ACKNOWLEDGMENTS

This work was supported by U.S. National Science Foundation Grant No. 90-24196 and MZT of Slovenia.

[1] J. C. Toledano, J. Schneck, and G. Errandonea, in *Incommensurate Phases in Dielectrics,* edited by R. Blinc and A. P. Levanyuk (Elsevier, Amsterdam, 1986), Vol. 2, p. 233, and references therein.

[2] J. Schneck, G. Calvarin, and J. M. Kiat, Phys. Rev. B **29**, 1476 (1984).

[3] H. Mashiyama, S. Tanisaki, and K. Hamano, J. Phys. Soc. Jpn. **51**, 2538 (1982).

[4] G. Errandonea, J. C. Toledano, J. Schneck, H. Savary, and J. Aubree, J. Phys. (Paris) Lett. **45**, L329 (1984).

[5] J. P. Jamet and P. Lederer, J. Phys. (Paris) Lett. **44**, L257 (1983).

[6] P. B. Jamieson, S. C. Abrahams, and J. L. Bernstein, J. Chem. Phys. **50**, 4352 (1969).

[7] W. F. Oliver and J. F. Scott, Ferroelectrics **117**, 63 (1991).

[8] A. M. Fajdiga, T. Apih, J. Dolinsek, R. Blinc, A. P. Levanyuk, S. A. Minyukov, and D. C. Ailion, Phys. Rev. Lett. **69**, 2721 (1992).

[9] R. Blinc and S. Zumer, Phys. Rev. B **41**, 11314 (1990).

[10] R. Blinc, T. Apih, J. Dolinsek, P. Prelovsek, J. Slak, D. C. Ailion, and K. Ganesan, Phys. Rev. B (to be published).

[11] J. Schneck, T. C. Toledano, C. Joffrin, J. Aubree, B. Joukoff, and A. Gabelotaud, Phys. Rev. B **25**, 1766 (1982).

[12] P. Bak, Rep. Prog. Phys. **45**, 587 (1982).

[13] R. Blinc, P. Prelovsek, A. Levstik, and C. Filipc, Phys. Rev. B **29**, 1508 (1984); P. Prelovsek and R. Blinc, J. Phys. C **17**, 577 (1984).

[14] K. Hamano, K. Ema, and S. Hirotsu, Ferroelectrics **36**, 343 (1981); R. Blinc, J. Dolinsek, P. Prelovsek, and K. Hamano, Phys. Rev. Lett. **56**, 2387 (1986).